Differential control of Yorkie activity by LKB1/AMPK and the Hippo/Warts cascade in the central nervous system

Ieva Gailite, Birgit L. Aerne, and Nicolas Tapon[1]

Apoptosis and Proliferation Control Laboratory, The Francis Crick Institute, Lincoln's Inn Fields Laboratory, London WC2A 3LY, United Kingdom

Edited by Ruth Lehmann, New York University Medical Center, New York, NY, and approved August 5, 2015 (received for review March 19, 2015)

The Hippo (Hpo) pathway is a highly conserved tumor suppressor network that restricts developmental tissue growth and regulates stem cell proliferation and differentiation. At the heart of the Hpo pathway is the progrowth transcriptional coactivator Yorkie [Yki–Yes-activated protein (YAP)/transcriptional coactivator with PDZ-binding motif (TAZ) in mammals]. Yki activity is restricted through phosphorylation by the Hpo/Warts core kinase cascade, but increasing evidence indicates that core kinase-independent modes of regulation also play an important role. Here, we examine Yki regulation in the *Drosophila* larval central nervous system and uncover a Hpo/Warts-independent function for the tumor suppressor kinase liver kinase B1 (LKB1) and its downstream effector, the energy sensor AMP-activated protein kinase (AMPK), in repressing Yki activity in the central brain/ventral nerve cord. Although the Hpo/Warts core cascade restrains Yki in the optic lobe, it is dispensable for Yki target gene repression in the late larval central brain/ventral nerve cord. Thus, we demonstrate a dramatically different wiring of Hpo signaling in neighboring cell populations of distinct developmental origins in the central nervous system.

Hippo | neuroblast | growth control | stem cells | development

The tight regulation of cell differentiation, proliferation, and death is crucial for the establishment of correct organ size during development. The conserved Hippo (Hpo) tumor suppressor pathway plays a central role in regulation of these processes (1, 2). The key effector of the Hpo pathway is the transcriptional coactivator Yki [Yes-activated protein (YAP)/transcriptional coactivator with PDZ-binding motif (TAZ) in mammals], which promotes the expression of a broad transcriptional program that includes proliferation/growth-promoting genes such as *cyclin E* (*cycE*), *myc*, and *bantam* microRNA (*ban*) and antiapoptotic genes such as death-associated inhibitor of apoptosis 1 (*diap1*) (3–7), as well as upstream Hpo pathway components such as *expanded* (*ex*), *kibra* (*kib*), and *four-jointed* (*fj*) (8–10). Overexpression of Yki/YAP/TAZ is sufficient to drive tissue growth in a number of contexts, and YAP/TAZ activation is frequently observed in solid tumors (11, 12). YAP and TAZ have recently been shown to regulate stem/progenitor cell proliferation and differentiation in several mammalian tissues (13–21). In flies, Yki has been implicated in regulation of proliferation of intestinal, follicle, and neuroepithelial progenitor cells (22–27).

Yki/YAP/TAZ activity is restrained through phosphorylation by the Hpo core kinase cascade, which is composed of the Ste20-like kinase Hpo (MST1/2 in mammals) and the Dbf2-related kinase Warts (Wts; LATS1/2 in mammals) (28–32). Upon activation by Hpo, Wts phosphorylates Yki on multiple residues, leading to its cytoplasmic retention (5, 33–39). Yki/YAP activity is regulated by a variety of upstream inputs, including systemic signals, cellular energy levels, cell polarity, and cell–cell contacts (1). However, the relative contribution of core kinase-dependent and independent mechanisms in the physiological regulation of Yki/YAP remains unclear (40).

Liver kinase B1 (LKB1) is a tumor suppressor kinase that regulates multiple processes such as cell polarity, proliferation, and stress responses (41). In humans, heterozygous mutation of *lkb1* leads to an increased benign and malignant tumor predisposition (Peutz-Jeghers syndrome) (42, 43), whereas sporadic mutations have also been linked to a variety of cancers (44–48). The main downstream targets of LKB1 are AMP-activated protein kinase (AMPK) family proteins, which LKB1 activates by phosphorylation of their activation loop (49). The best-characterized substrate of LKB1 is AMPK itself, which acts as an intracellular energy sensor (50). Under low-energy conditions, AMPK is activated by AMP binding, resulting in conformational changes that promote activatory phosphorylation by LKB1 (51). When activated, AMPK restores energy balance by promoting energy-efficient ATP generation through oxidative phosphorylation and antagonizing ATP-expending anabolic processes such as gluconeogenesis and fatty acid synthesis (52).

Recently, both LKB1 and AMPK have been reported to repress YAP activity in mammalian cell culture and cancer models (53–57), either by modulating the core kinase cascade or via direct phosphorylation of YAP by AMPK. Here, we find that loss of LKB1 leads to Yki activation and accelerated proliferation in the *Drosophila* larval central brain (CB) and ventral nerve cord (VNC). LKB1-mediated inhibition of Yki activity is independent of the Hpo/Wts kinase cascade and is mediated by AMPK,

Significance

The correct regulation of tissue growth in developing organisms is essential for functional organ formation. The evolutionarily conserved transcriptional coactivator Yorkie (Yki)/Yes-activated protein (YAP) responds to a variety of upstream inputs to promote tissue growth. Yki/YAP is known to regulate stem cell proliferation, thus affecting final organ size. The Hippo (Hpo)/Warts kinase cascade is a key inhibitor of Yki activity in many epithelial tissues. Here, we show that Yki is inhibited by the nutrient-sensing liver kinase B1 (LKB1)/AMP-activated protein kinase (AMPK) cascade independent of Hpo/Warts in a population of neural progenitors in the developing *Drosophila* larval brain. Our results suggest a tissue-specific nutrient-dependent mode of Yki activity regulation. Furthermore, a tissue-specific differential wiring of Hpo signaling could represent an adjustment to the proliferation requirements of different tissue types.

Author contributions: I.G. and N.T. designed research; I.G. and B.L.A. performed research; I.G. and N.T. analyzed data; and I.G. and N.T. wrote the paper.

The authors declare no conflict of interest.

This article is a PNAS Direct Submission.

Freely available online through the PNAS open access option.

[1]To whom correspondence should be addressed. Email: nic.tapon@crick.ac.uk.

This article contains supporting information online at www.pnas.org/lookup/suppl/doi:10.1073/pnas.1505512112/-/DCSupplemental.

suggesting a potential energy-dependent pathway controlling proliferation in the CB and VNC.

Results

***lkb1* Regulates Hpo Signaling in the Optic Lobe.** *Drosophila* neural stem cells or neuroblasts (NBs) have been extensively studied as a model for stem cell proliferation and differentiation (58, 59). The developing *Drosophila* larval brain consists of two compartments of different developmental origins: the optic lobe (OL) and the CB/VNC (Fig. 1*A*). The CB/VNC is formed by NBs that delaminate from the embryonic neuroectoderm at stages 8–11 (60, 61). In contrast, the OL invaginates as a neuroepithelial sheet from the posterior procephalic region in stage 11 embryos and later separates into the inner optic anlagen and the outer optic anlage. The outer optic anlage cells remain neuroepithelial until their conversion to medulla NBs during the third instar larval stage by a wave of differentiation initiated at the medial margin of the neuroepithelium (Fig. 1*B*) (62–64). Most adult neurons are specified during larval development; thus, regulation of larval NB proliferation is crucial for the correct development of the adult nervous system.

To test the role of *lkb1* in the regulation of cell proliferation in *Drosophila*, we analyzed larvae homozygous for the *lkb1* loss-of-function mutation $lkb1^{x5}$. Mutant larvae can survive up to early pupal stages and exhibit overgrowth of the central nervous system (CNS) at the white prepupal stage (Fig. 1 *C*–*E*), as described previously (65). To analyze the brain overgrowth phenotype in more detail, we quantified the volume of the VNC and OL compartments separately. We observed a marked overgrowth of both compartments (Fig. 1*E*). Whole mutant $lkb1^{x5}$ larval third instar CBs exhibited an increased number of mitotic cells positive for phosphohistone H3 (PH3) compared with heterozygous $lkb1^{x5}$/+ controls, indicating increased proliferation (Fig. 1*F*). We also observed a mild increase in the total number of Dpn-positive NBs in $lkb1^{x5}$ whole mutant larval CBs (Fig. 1*G*), suggesting the loss of *lkb1* function might affect NB asymmetric cell division. Indeed, *lkb1* mutations have been reported to elicit multiple defects in NB asymmetric divisions (66). However, this phenotype is mild in comparison with those of other proteins involved in regulating NB asymmetric cell division, such as Lgl, Brat, aPKC, and AurA (67–72).

Hpo pathway disruption or Yki overexpression in the OL neuroepithelium leads to overproliferation and OL overgrowth (23, 73). To test whether *lkb1* functions in the Hpo pathway in the OL, we generated *lkb1* mutant clones in the larval third instar brains. Clones mutant for $lkb1^{x5}$ in the OL are generally reduced

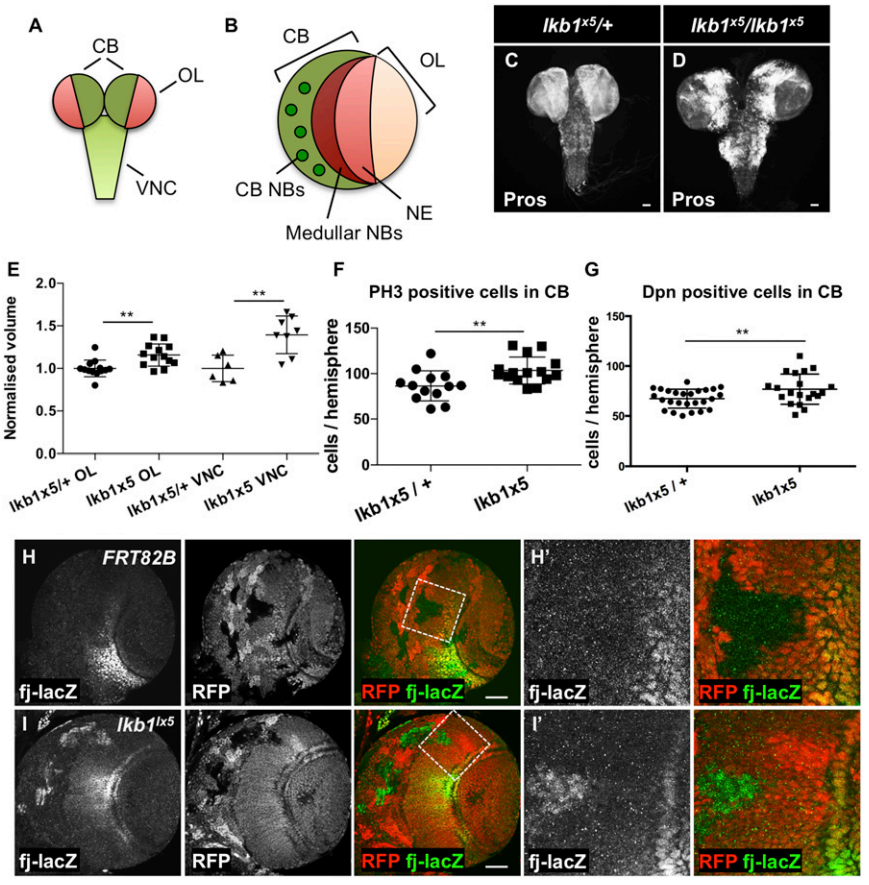

Fig. 1. Loss of *lkb1* function causes overgrowth of the larval brain. (*A*) Schematic representation of the compartments of the larval CNS. (*B*) Schematic representation of the third instar larval brain hemisphere. CB, central brain; NB, neuroblasts; NE, neuroepithelium; OL, optic lobe; VNC, ventral nerve cord. (*C* and *D*) CNS morphology of $lkb1^{x5}$/+ (*C*) and $lkb1^{x5}/lkb1^{x5}$ (*D*) white prepupae. Pros staining labels neuronal cells. (*E*) Volume of $lkb1^{x5}$ homozygous VNCs ($n = 8$) and OLs ($n = 13$) is increased in comparison with heterozygous $lkb1^{x5}$/+ VNCs ($n = 6$) and OLs ($n = 13$). Brains were dissected from white prepupae. (*F*) $lkb1^{x5}$ homozygous third instar larval brains ($n = 15$) have increased PH3-positive cell numbers in the CB in comparison with $lkb1^{x5}$/+ controls ($n = 13$). (*G*) $lkb1^{x5}$ homozygous third instar larval brains ($n = 20$) show an increase in Dpn-positive cell numbers in the CB in comparison with $lkb1^{x5}$/+ controls ($n = 26$). $^{**}P < 0.01$. Statistical significance was analyzed using Student's *t* test. (*H* and *H'*) Heat shock (hs) FLP/FRT-generated $lkb1^{x5}$ clones have increased *fj-lacZ* levels in the OL (*H* and *H'*) in comparison with the control clones (*I* and *I'*). Higher magnifications of the boxed areas are shown in *H'* and *I'*. Clones are marked by the absence of the Red Fluorescent Protein (RFP) expression. (Scale bars, 50 μm.)

in size and frequency (Fig. 1 *H* and *I*). The Yki-sensitive *fj-lacZ* transcriptional reporter is expressed in a radial pattern with increased expression levels in the center of the OL (Fig. 1 *H* and *H′*) (23). We observed an increase of *fj-lacZ* expression in $lkb1^{x5}$ clones in the area of OL normally exhibiting a low level of *fj* expression (Fig. 1 *I* and *I′*). Thus, loss of *lkb1* function can induce Yki target gene expression in the OL.

***lkb1* Restricts Yki Activity in the CB.** Although the role of Yki and the Hpo core kinase cascade in the OL has previously been described (23, 73), little is known about Yki function in the CB. Immunostainings of third instar larval CNSs revealed that the Yki targets Ex, DIAP1, and Kib are expressed in the CB at levels comparable to in the OL (Fig. 2 *A*, *C*, and *E* and Fig. S1*A*). Strikingly, $lkb1^{x5}$ mutant clones in the CB exhibited strongly increased protein levels of Ex, Kib, and DIAP1, as well as increased levels of the *ex-lacZ* and *fj-lacZ* transcriptional reporters (Fig. 2 *B*, *D*, *F*, *H*, Fig. S1*B*, and Fig. 1 *H* and *I*), but not of the Notch activity reporter *E(spl)m8-lacZ* (Fig. S1*E*). Mutant clones of a different *lkb1* allele, $lkb1^{4A4\text{-}2}$, caused by a deletion of the first 145 amino acids (74), displayed a similar up-regulation of Yki targets (Fig. S1*F*). We also observed increased amounts of Kib protein in $lkb1^{x5}$ clones in the VNC (Fig. S1*G*). Activation of Yki induces expression of E2F1, a transcription factor involved in cell cycle regulation and G1–S transition (75, 76). Consistently, we observed increased E2F1 protein levels in $lkb1^{x5}$ MARCM (mosaic analysis with a repressible cell marker) clones (Fig. S1 *C* and *D*).

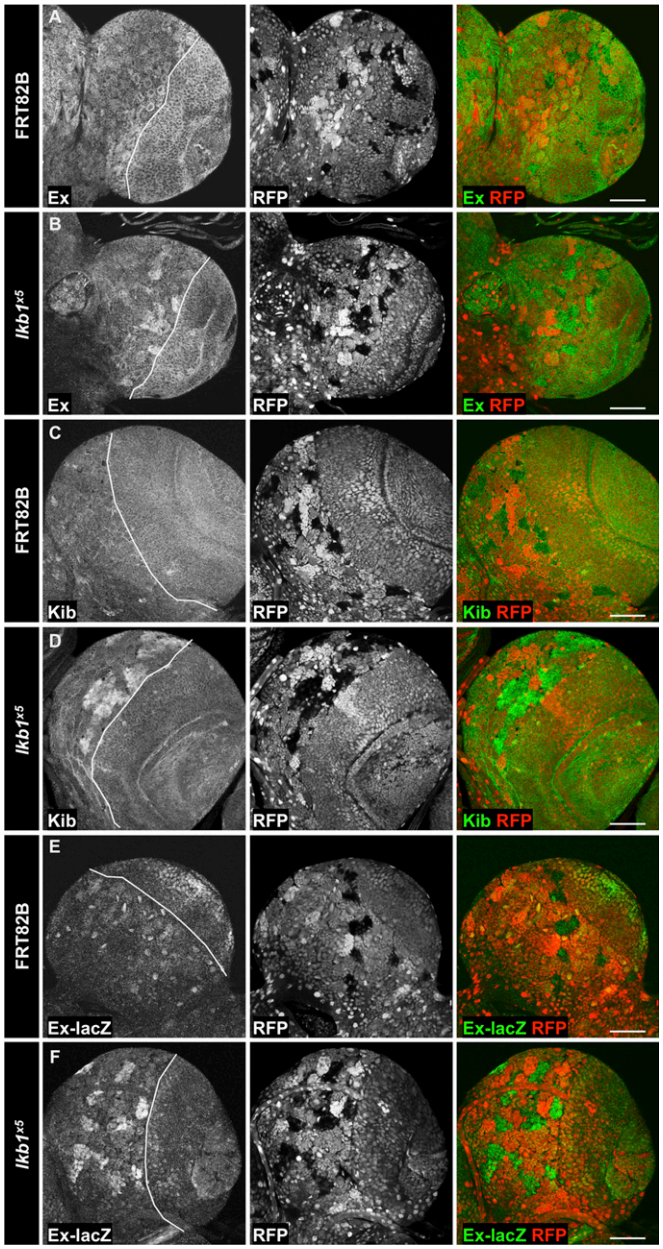

Fig. 2. *lkb1* restricts Yki target expression in the larval CB. Expression levels of the Yki targets Ex (*B*), Kib (*D*), and the transcriptional reporter *ex-lacZ* (*F*) are elevated in hsFLP/FRT-generated *lkb1* mutant clones in the CB of third instar larvae compared with wild-type clones (*A*, *C*, and *E*). Clones are marked by the absence of RFP expression. OL and CB compartments are separated by a line. (Scale bars, 50 μm.)

We wished to determine whether Yki target up-regulation upon *lkb1* loss occurs in both the CB NBs and their progeny. We therefore generated MARCM mutant clones positively marked with GFP (Fig. 3 *A*–*H*). Most CB NBs are type I NBs and divide asymmetrically to self-renew and produce a smaller ganglion mother cell, which divides once more to give rise to two neurons or glial cells. Eight type II NBs, which have a different lineage, are located in the posterior side of the CB. Type II NBs give rise to intermediate neural progenitors, which, after a maturation phase, divide asymmetrically three to five times to produce another intermediate neural progenitor and a ganglion mother cell (58). In control MARCM clones, the Yki targets Kib and DIAP1 were expressed uniformly in the NBs (marked by Dpn) and their progeny (Fig. 3 *A*, *C*, *E*, and *G*). Kib protein levels were clearly increased in both $lkb1^{x5}$ mutant NBs and their progeny (Fig. 3 *B* and *F*). Interestingly, DIAP1 levels were increased in the progeny of both type I and type II NBs, but only type I NBs up-regulated DIAP1 (Fig. 3*D*), whereas type II NBs maintained wild-type DIAP1 levels (Fig. 3*H*). The difference in DIAP1 expression between type I and type II NBs might be caused by differences in gene expression between these cell types (67, 77, 78). Finally, we observed a dramatic increase in Yki nuclear localization in $lkb1^{x5}$ mutant NBs (92.2%) in comparison with control NBs (9.1%; Fig. 3*I*), correlating with increased expression of Yki target genes.

***lkb1* Loss Accelerates Cell Division and Tissue Growth.** Because $lkb1^{x5}$ whole mutant brains exhibited an increase in the total number of Dpn-positive cells, we analyzed the number of Dpn-expressing cells in MARCM clones of type I NBs (Fig. 3*J*). In agreement with the previously described role of LKB1 in regulating NB asymmetric cell divisions (66), $lkb1^{x5}$ MARCM clones had an increased incidence of clones containing two Dpn-positive cells (21.8%) compared with 2.5% in control clones, possibly caused by asymmetric NB division defect or a failure in ganglion mother cell differentiation. To investigate whether excess Yki activity is responsible for the increased NB number in *lkb1* mutants, we depleted *yki* by RNAi in $lkb1^{x5}$ MARCM clones. *yki* knockdown had no effect on NB numbers in $lkb1^{x5}$ clones: 23.5% of clones contained two Dpn-positive cells. In addition, *yki* depletion alone did not significantly affect NB numbers, as 95.7% of clones had a single Dpn-positive cell. These results suggest that LKB1 regulates Yki activity independent of its role in asymmetric cell division.

Yki activation leads to increased cell proliferation in a variety of tissues (79). To test whether the rate of cell division is accelerated by *lkb1* loss in the larval CNS, we analyzed PH3 staining in the third instar larval VNC. MARCM clones mutant for $lkb1^{x5}$ (Fig. 3*K*) exhibited a larger proportion of clones with at least one dividing cell, as well as an increased mean number of dividing cells per clone (1.46 in $lkb1^{x5}$ clones vs. 1.12 in the control clones). Extending our analysis to individual cell types,

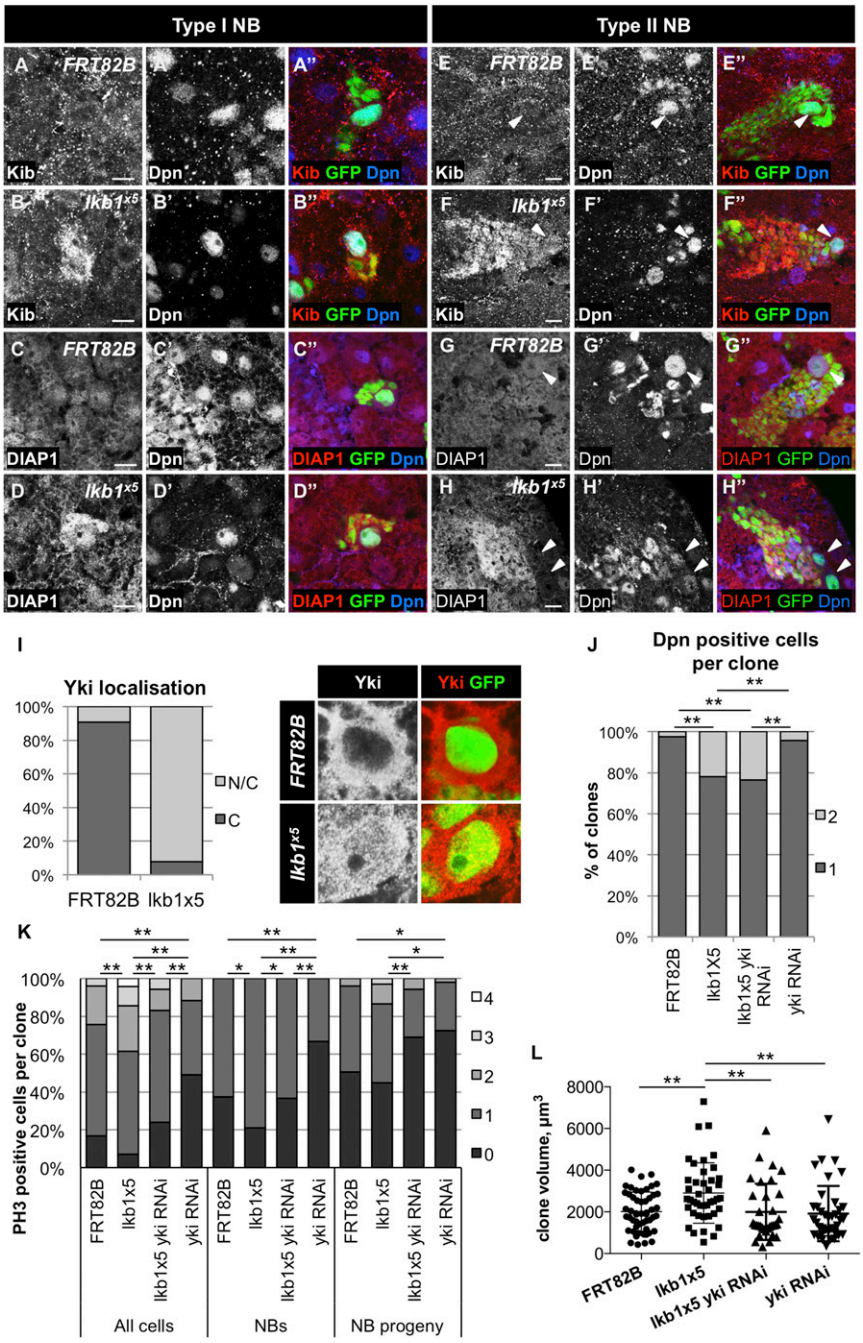

Fig. 3. Yki target gene expression in *lkb1* mutant NBs and their progeny. Expression of Yki target genes in MARCM clones of type I NBs (*A*–*D*′′) and type II NBs (*E*–*H*′′). anti-Dpn staining marks type I NBs in *A*–*D*′) and type II NBs and mature intermediate neural progenitors in *E*–*H*′. Type II NBs are marked by arrowheads in *E*–*H*′. Kib (*A* and *E*) and DIAP1 (*C* and *G*) are uniformly expressed both in NBs and their progeny in control MARCM clones. Protein levels of Kib (*B* and *F*) are increased both in type I and type II NBs and their progeny in *lkb1*^{x5} MARCM clones. (*D* and *H*) In *lkb1*^{x5} mutant clones, DIAP1 protein levels are increased in type I NBs and in the type I and type II NB progeny, but not in the type II NBs (*H*). Clones are marked by GFP expression. (Scale bars, 10 μm.) (*I*) Quantification of Yki localization in NBs of MARCM clones of the indicated genotypes in third instar larval CB. C, cytoplasmic Yki; N/C, cytoplasmic and nuclear Yki. $n = 66$ (*FRT82B*), 64 (*lkb1*^{x5}). (*J*) Quantification of Dpn-positive cells in type I NB MARCM clones of the indicated genotypes 48 h after clone induction in the CB of third instar larvae. $n = 46$ (FRT82B and *yki* RNAi), 57 (*lkb1*^{x5}), 51 (*lkb1*^{x5} *yki* RNAi). (*K*) Quantification of PH3-positive cells in MARCM clones of the indicated genotypes in type I NB lineages in the third instar larval VNC. $n = 78$ (FRT82B), 69 (*lkb1*^{x5}), 71 (*lkb1*^{x5} *yki* RNAi), 51 (*yki* RNAi). (*L*) Quantification of the volume of MARCM clones of the indicated genotypes 72 h after induction in the third instar larval VNC. $n = 52$ (FRT82B), 42 (*lkb1*^{x5}), 33 (*lkb1*^{x5} *yki* RNAi), 38 (*yki* RNAi). $^{*}P < 0.05$; $^{**}P < 0.01$. Statistical significance was analyzed using X^2 test in *J* and Student's *t* test in *K* and *L*.

we observed an increased incidence of dividing NBs in *lkb1*^{x5} clones (0.79 in comparison with 0.63 in control clones), as well as an increased number of dividing NB progeny in *lkb1*^{x5} clones (0.72 vs. 0.53 in control clones). *yki* depletion rescued the increased cell division of *lkb1*^{x5} cells (1.0 dividing cell per clone), with both NB proliferation (0.6 dividing NBs per clone) and NB progeny (0.37 dividing cells per clone) mitotic indices being reduced. Expression of *yki* RNAi alone decreased the average number of dividing cells per clone to 0.63, with 0.33 dividing NBs and 0.29 dividing NB progeny per clone. Therefore, loss of *lkb1*

increases the number of mitotic cells in a Yki-dependent manner in the VNC.

Next, we assessed whether the increased mitotic index in *lkb1* clones resulted in increased clone growth. We measured clone volume in MARCM clones in the third instar VNC 72 h after clone induction. In line with the mitotic indices, we observed a significant increase in the mean volume of $lkb1^{x5}$ clones compared with controls (Fig. 3*L*). Knockdown of *yki* in $lkb1^{x5}$ clones reduced the clone volume back to control levels (Fig. 3*L*). Together, these results show that loss of *lkb1* function in the larval CNS leads to increased Yki target gene expression, increased cell division rates, and tissue growth.

LKB1 Gain of Function Inhibits Yki Activity and Proliferation in the CB. To analyze the effect of LKB1 overexpression on Yki activity in the CB, we used the *optix-Gal4* driver line that drives gene expression in a subset of type II NBs and their progeny in the CB, as well as in a subset of OL cells (80, 81). LKB1 overexpression alone resulted in cell death; therefore, we coexpressed caspase inhibitor p35 in the compartment. LKB1 overexpression reduced Ex protein levels in the *optix* compartment (Fig. 4 *A*–*D*). Accordingly, we observed a decreased number of PH3-positive mitotic cells upon LKB1 overexpression (Fig. 4 *E*–*G*), suggesting decreased proliferation. To test the effects of LKB1 overexpression in the whole CB, we used a P-element insertion carrying the *Gal4* coding sequence [*P(GawB)NP5443*] that is expressed specifically in the CB compartment and the VNC, as well as in the lamina (Fig. 4*H*). Overexpression of LKB1 under the control of *P(GawB)NP5443* led to a significant reduction in CB volume in comparison with GFP overexpression (Fig. 4 *H*–*J*). Similarly, overexpression of LKB1 in the OL with the *c855a-Gal4* driver line reduced OL volume (Fig. 4 *K*–*M*). Thus, increasing LKB1 levels is sufficient to cause a reduction in Yki activity and tissue growth in the larval CB.

Loss of Hpo/Wts Activity Does Not Affect Yki Target Gene Expression in the CB. Because Yki upstream regulation in the larval CB has not previously been examined, we analyzed the effects of Hpo core kinase cascade inhibition in the third instar larval CB. We analyzed expression levels of Yki target genes in *wts* mutant clones and clones expressing Yki^{S168A}, which cannot be inhibited by Wts phosphorylation (Fig. 5). In both cases, we observed a clear increase in expression of *ex-lacZ* transcriptional reporter (Fig. 5 *B* and *B″*) and Ex protein levels in the OL (Fig. 5 *C* and *C″*) in comparison with the control situation (Fig. 5 *A* and *A″*). Surprisingly, no changes in Yki target expression were observed in CB clones (Fig. 5 *B′* and *C′*). These results are consistent with previous observations that Yki^{S168A} activates target genes only in

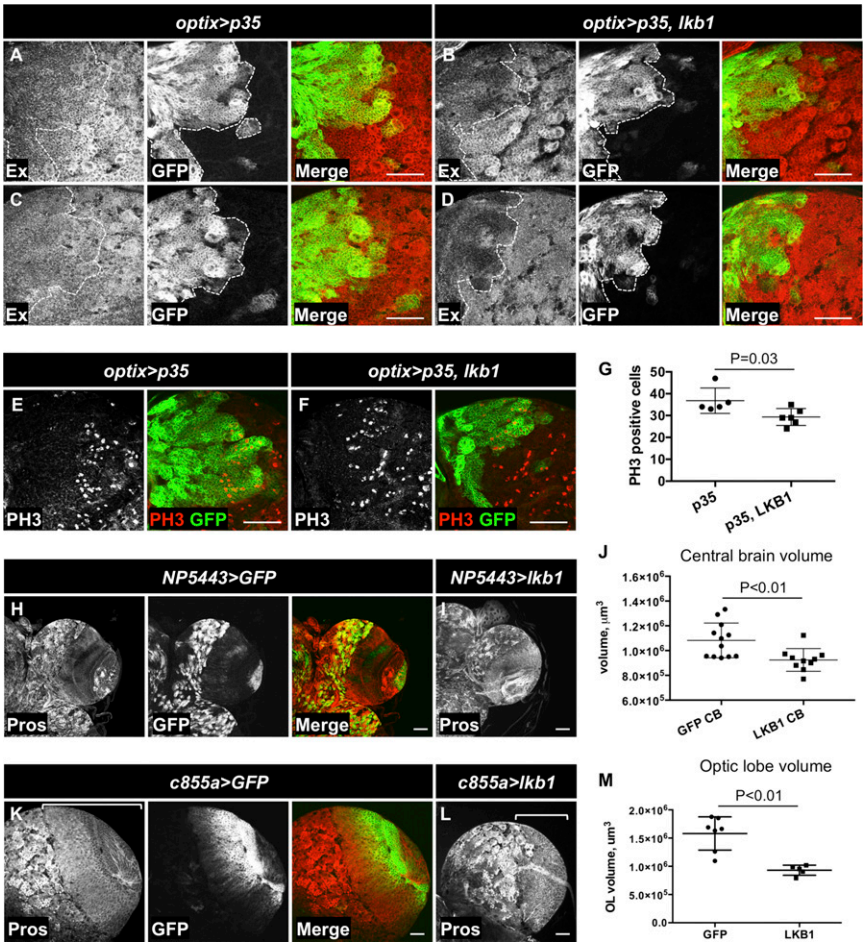

Fig. 4. LKB1 reduces Yki target gene expression and growth in the CB. (*A*–*D*) Overexpression of LKB1 under the control of *optix-Gal4* in a subset of CB NBs and their progeny reduces protein levels of Kib and Ex. The caspase inhibitor p35 was coexpressed to prevent cell death upon LKB1 over-expression. (*E*–*G*) Overexpression of LKB1 reduces the number of PH3-labeled mitotic cells in the *optix* compartment of the CB. The *optix* compartment is marked by GFP expression in *A*–*F*. (*H*) Expression pattern of *P(GawB)NP5443* in the CB of white prepupae. (*I* and *J*) Overexpression of LKB1 in the CB reduces its volume. Pros staining labels neuronal cells in the CB. (*K*–*M*) Overexpression of LKB1 in the OL using *c855a-GAL4* reduces its volume. The OL compartment in *K* and *L* is marked with a bracket. (Scale bars, 50 μm.) Statistical significance was analyzed using a Student's *t* test in *G*, *J*, and *M*.

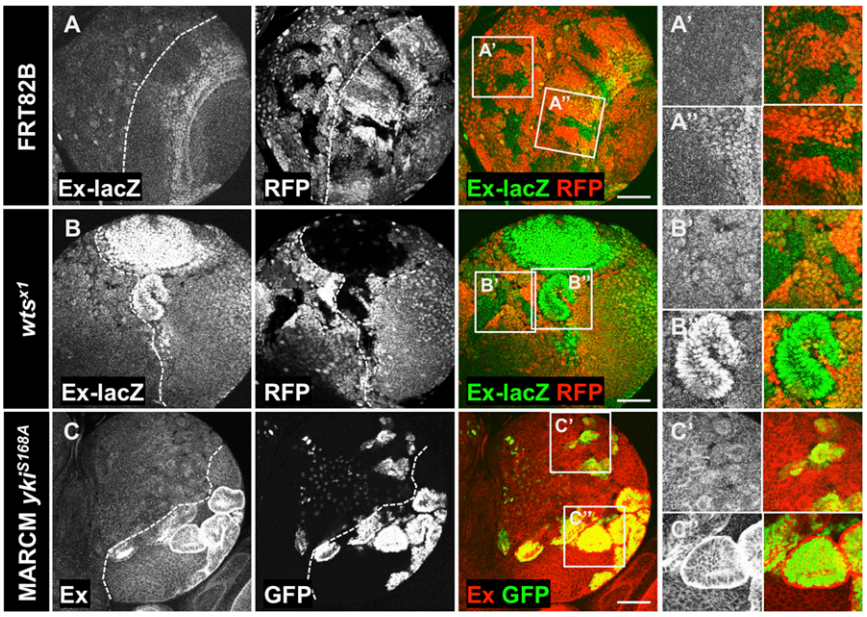

Fig. 5. Wts is dispensable for Yki inhibition in the CB. (*A* and *B*) Expression of *ex-lacZ* transcriptional reporter in control (*A*–*A*′′) or wts^{x1} (*B*–*B*′′) mutant clones. Loss of *wts* function increases expression of *ex-lacZ* transcriptional reporter in the OL (*B*′′) in comparison with the control clones (*A*′′), but not in the CB (*B*′). *ex-lacZ* expression in the control clones in the CB is shown in (*A*′). Clones are marked by absence of RFP. MARCM clones overexpressing Yki^{S168A} (*C*–*C*′′) induce accumulation of Ex protein in the OL (*C*′′), but not in the CB (*C*′). Clones are marked by GFP expression. OL and CB areas are separated by a dashed line in *A*, *B*, *C*, and *D*. Insets show magnifications of the boxed areas. (Scale bars, 50 μm.)

the NE (23) and suggest that Yki is repressed by a Hpo/Wts-independent mechanism in the CB. In addition, overexpression of the activated $Yki^{S111A\ S168A\ S250A}$ (Yki^{3SA}—mutant for all three Wts sites) induced Kib accumulation and overgrowth in the OL, but not in the CB (Fig. S2 *A* and *C*). Ex has been shown to inhibit Yki independent of Wts by sequestering it at the plasma membrane (82, 83). However, we did not observe changes of Kib protein levels in ex^{e1} mutant clones in the brain (Fig. S3*A*), suggesting Ex does not restrain Yki activity in the CB.

LKB1 Regulates Yki Activity Downstream from, or Parallel to, Wts. Next, we sought to position LKB1 activity in Yki regulation in the context of known Yki regulators. Overexpression of *UAS-hpo* in $lkb1^{x5}$ MARCM clones did not rescue the increase of Ex levels in the cells (Fig. 6 *A*–*C*), suggesting *lkb1* acts downstream or in parallel to Hpo. As expected, *yki* RNAi expression prevented Ex up-regulation upon *lkb1* loss in the CB (Fig. 6*D*). Finally, *UAS-wts* overexpression reduced Ex levels in $lkb1^{x5}$ clones (Fig. 6*E*), showing that ectopically expressed Wts is able to repress Yki activation induced by the loss of *lkb1* function in the CB. Together with the *wts* loss of function data (Fig. 5 *B* and *B*′′), this suggests that Wts may not be expressed in the CB, although *hpo* and *wts* transcripts are detectable in NBs (84). Alternatively, Wts could be inactive in the larval CB in late developmental stages, or its Yki-repressing activity may be overridden by that of LKB1, which acts in parallel to restrain Yki. Moreover, we observed that in the NE, where loss of *wts* results in increased Ex protein levels, overexpression of LKB1 can restore Ex expression to wild-type levels (Fig. S2 *E* and *F*). This suggests that LKB1 inhibits Yki independent of Wts. LKB1 overexpression can reduce Kib levels in the CB even when activated Yki^{3SA} is expressed (Fig. S2*B*). Furthermore, Yki^{3SA}-V5 nuclear localization in CB NBs is increased from 23.9% to 82.4% of NBs when *lkb1* is mutated (Fig. S2*G*), indicating that LKB1 can inhibit Yki independent of Wts in the CB. However, overexpression of LKB1 together with Yki^{3SA} is not sufficient to restore Kib levels to normal in the OL (Fig. S2 *C* and *D*). This result suggests that the ability of LKB1 to inhibit Yki activity may vary in different tissues. Alternatively, it may be a result of the high levels of Yki^{3SA} expression in MARCM clones in the optic lobe.

AMPK Acts Downstream of LKB1 in the CB. To further probe the function of LKB1 in the CB, we analyzed the role of known downstream targets of LKB1. LKB1 has been described to regulate YAP in mammals via the basolateral cell polarity proteins Par-1 and Scrib (53). However, we did not observe any changes of Ex protein levels in mutant clones for the $par\text{-}1^{w3}$ and $scrib^{2}$ loss-of-function alleles in the CB (Fig. S3 *B* and *C*). In addition, it has previously been observed that Scrib localization in NBs is not affected by *lkb1* loss (85). LKB1 has been shown to regulate the asymmetric NB division via suppressor-of-G2-allele-of-skp1 (Sgt1) (85), but we did not observe any changes in Ex protein levels in $sgt1^{S2383}$ mutant clones (Fig. S3*D*).

AMPK is one of the best characterized downstream targets of LKB1 in regulation of a variety of processes, including the regulation of energy metabolism and cell division (86). Indeed, *ampk* loss-of-function clones exhibited accumulation of the Yki targets Ex and Kib (Fig. 7 *A* and *B*). Although mild depletion of *ampk* using RNAi in the *optix* compartment was not sufficient to visibly affect DIAP1 levels (Fig. 7*E* and Fig. S4*A*), *ampk* RNAi rescued the reduction in DIAP1 levels caused by LKB1 overexpression (Fig. 7 *C*–*F* and Fig. S4*B*). These results suggest that AMPK acts downstream of LKB1 in regulating Yki activity in the CB.

AMPK activates a range of downstream targets involved in regulation of protein synthesis, metabolism, cytoskeleton regulation, and autophagy (86). However, genetic manipulation of previously characterized downstream targets of AMPK, including dTORC, TSC1/2, ACC, FOXO, Raptor, Atg1, CREB, Sqh, SREBP, HDAC4, dCBP, and Rheb, did not induce detectable changes in Yki target expression in CB (Fig. S4 *C* and *D*). Very recently, AMPK was shown to phosphorylate YAP directly in mammalian cells (56, 57). We performed an in vitro kinase assay with purified Yki and human AMPK and LKB1 (Fig. S4*E*). Yki phosphorylation was increased in samples

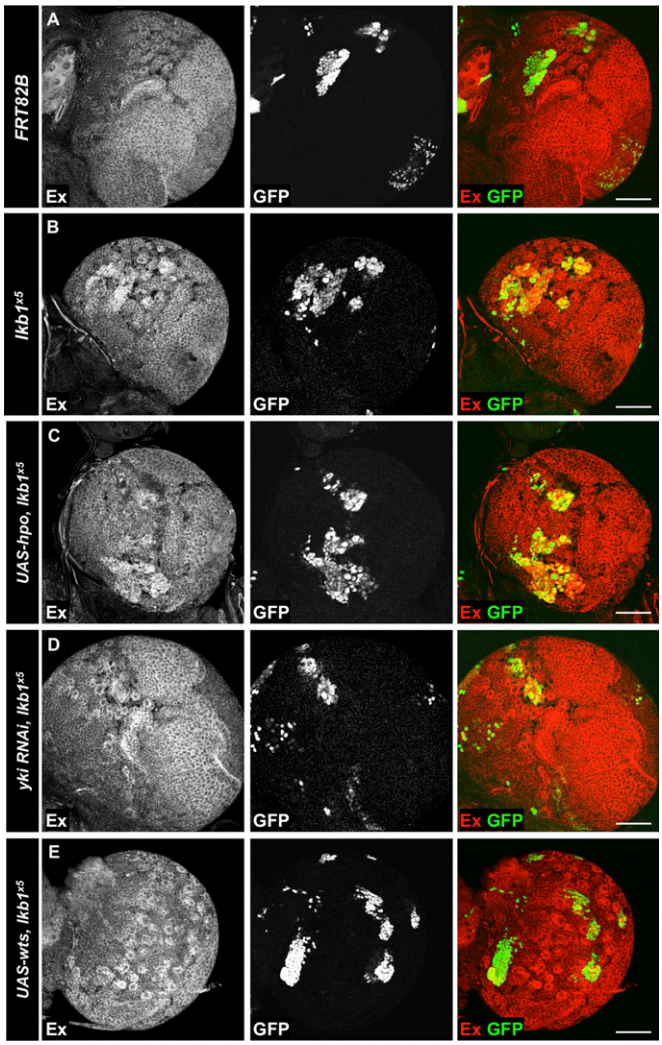

Fig. 6. *lkb1* regulates Yki target genes downstream of *wts*. (*A*–*E*) MARCM clones in third instar larval CBs. (*A*) Ex protein levels in control clones. (*B*) $lkb1^{x5}$ mutant clones accumulate Ex. (*C*) Overexpression of *UAS-hpo* does not rescue up-regulation of Yki targets. Expression of *UAS-yki RNAi* (*D*) or *UAS-wts* (*E*) rescues Ex accumulation caused by loss of *lkb1* function. Clones are marked by GFP expression. (Scale bars, 50 μm.)

containing AMPK, suggesting the direct regulation of Yki by AMPK might be conserved between flies and mammals.

Discussion

Hpo Kinase Cascade-Dependent or Independent Yki/YAP Regulation by LKB1/AMPK. Here, we identify a function for the energy-sensing module LKB1/AMPK in restraining the activity of the Hpo pathway effector Yki in the larval neuronal stem cells of the CB and VNC. Although several recent reports suggest that mammalian YAP also responds to LKB1 and/or AMPK, a number of distinct Hpo/Wts-dependent and independent mechanisms have been proposed. Although Nguyen et al. describe an AMPK-independent and partially LATS-independent pathway for YAP inhibition by LKB1 (54), Mohseni et al. show that LKB1 acts via microtubule affinity-regulating kinase 1 (MARK1)/Par-1 to promote the localization of the polarity determinant Scrib, which in turn has been proposed to scaffold the Hpo core kinase cascade (19, 53). In contrast, three recent studies suggest that AMPK may be a key YAP regulator downstream of LKB1 (55–57). First, AMPK can inhibit YAP by phosphorylating and stabilizing the junctional protein angiomotin-like 1 (AMOTL1), thereby promoting YAP inhibitory phosphorylation by LATS1 (55). Second, energy stress reduced YAP activity both via AMPK-mediated induction of Lats1/2 activity and also through direct phosphorylation of YAP by AMPK (55–57). The outcome of YAP phosphorylation by AMPK [reduced binding to TEAD (TEA-domain) transcription factors or a distinct mechanism], as well as the sites involved, vary between the two studies (56, 57).

Our data suggest that, at least in the *Drosophila* CNS, LKB1/AMPK act in parallel to Hpo/Wts to repress Yki transcriptional activity, according to several lines of evidence. First, loss of LKB1/AMPK strongly de-repressed Yki targets in the CB/VNC (Fig. 2), whereas loss of Wts had no such effect (Fig. 5). Second, increasing Wts expression in *lkb1* mutant tissue in the CB suppressed Yki activity (Fig. 6*E*), and vice versa, LKB1 overexpression suppressed Yki activity in *wts* mutant tissue in the OL (Fig. S2 *E* and *F*). Finally, misexpression of Yki mutants for the inhibitory Wts sites (Yki^{S168A} and Yki^{3SA}), which potently induce Yki target genes in the OL, are transcriptionally inert in CB NBs (ref. 23 and Fig. 5*C* and Fig. S2*C*). This suggests that an alternative Wts-independent Yki inhibitory influence acts in the

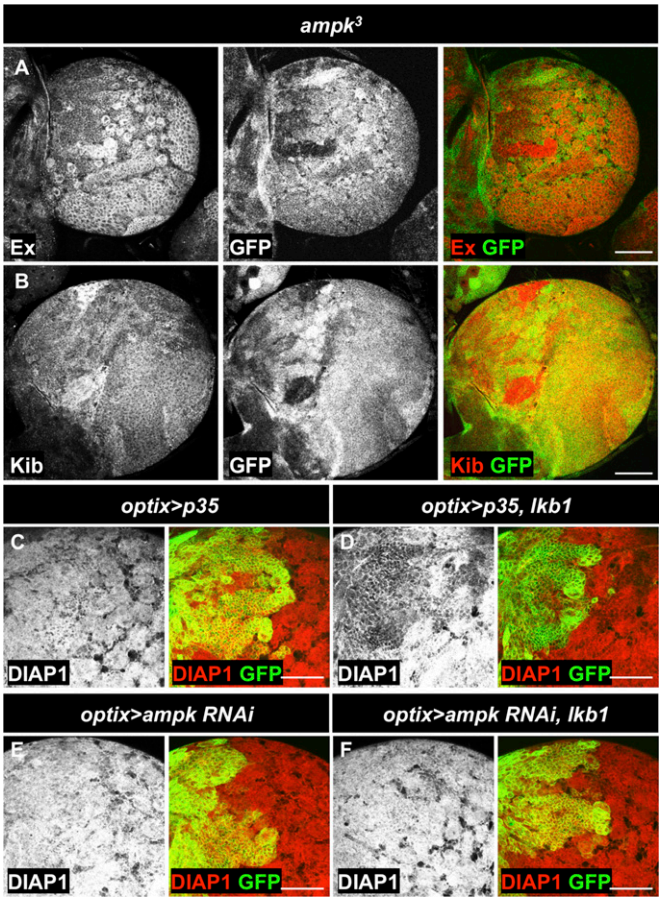

Fig. 7. Loss of *ampk* function up-regulates Yki target genes. (*A* and *B*) Protein levels of Kib and Ex are increased in hsFLP/FRT-generated $ampk^{3}$ clones. Clones are marked by the absence of GFP expression. (*C*–*F*) RNAi against *ampk* rescues inhibition of Yki target gene expression by LKB1. LKB1 overexpression in the *optix* compartment (*D*) reduces DIAP1 protein levels in comparison with the control (*C*). The caspase inhibitor p35 was coexpressed to prevent cell death upon LKB1 over-expression in (*C* and *D*). (*E*) Expression of *UAS-ampk* $RNAi^{GD736}$ alone does not modify DIAP1 levels. (*F*) Expression of *UAS-ampk* $RNAi^{GD736}$ together with *UAS-lkb1* rescues the reduction of DIAP1 levels. The *optix* compartment is marked by GFP expression in *C*–*E*. (Scale bars, 50 μm.)

CB/VNC, mediated by LKB1/AMPK. Our in vitro phosphorylation data are consistent with a direct role for AMPK in repressing Yki through phosphorylation (Fig. S4*E*), although further work will be required to establish in vivo relevance of this phosphorylation in NBs and whether the phosphorylation sites are conserved in mammals.

Energy-Dependent Regulation of Yki/YAP. AMPK acts as a sensor of intracellular energy levels and acts to inhibit anabolic processes with a high energy cost and promoting energy-generating catabolic processes. For example, AMPK inhibits protein and lipid synthesis and gluconeogenesis while promoting glucose transport, glycolysis, fatty acid oxidation, and autophagy (87). Interestingly, energy stress elicited by glucose withdrawal/2-deoxy-glucose treatment or the AMPK activator metformin led to YAP inactivation and reduced tumor cell growth both in cell culture and in xenograft experiments, even in cells lacking LATS1/2 (55–57). A tissue-specific role of AMPK in regulation of Yki activity in the CB/VNC may therefore reflect the need for adjustment of proliferation rates of different tissues under low energy conditions, although the *Drosophila* larval nervous system is also buffered from systemic nutrient restrictions during late larval development through a process known as sparing (88). In mammals, YAP promotes the expression of the glucose transporter GLUT3 (57), suggesting it can in turn affect energy metabolism.

Yki Regulation in Epithelia and Asymmetrically Dividing Neuronal Stem Cells. An important aspect of this work is the demonstration that two related, but developmentally distinct, populations of neural stem cells use dramatically different strategies to restrict Yki activity during their larval proliferative phase. Although both Hpo/Wts and LKB1 restrict Yki activity in the OL, LKB1/AMPK play the major role in CB/VNC neuroblasts. Although both the CB/VNC and the OL NBs ultimately originate from neuroepithelia, the former delaminate during embryonic development, whereas the latter remain neuroepithelial until the larval stages, when Hpo and Notch pathways regulate the epithelial to neuroblast transition (23). This behavioral difference may therefore form the basis for a fundamental difference in the regulation of Yki/YAP in epithelial cells versus nonepithelial asymmetrically dividing stem cells. Indeed, much evidence indicates that epithelial cell–cell junctions act as an important site for Yki/YAP regulation (89). It will therefore be interesting to examine the interplay between LKB1/AMPK and Hpo/Wts in Yki/YAP regulation in other stem cell populations such as vertebrate adult neural stem cells or intestinal stem cells. Is the LKB1/AMPK module generally important in epithelia to restrict Yki/YAP activity? Although *lkb1* mutant clones in epithelial cells generally do not overgrow (90), this may be a result of disruption of apicobasal polarity in these cells, which is a well-characterized consequence of LKB1 loss that may mask overproliferation phenotypes (74, 91–93).

Experimental Procedures

Immunohistochemistry. For clonal analysis with either FRT/FLP or MARCM systems, clones were induced by a 1-h or 30-min heat shock at 37 °C in 24–48 h after-egg-laying larvae. Brains of third instar larvae or white prepupae were dissected, fixed for 20 min in 4% (wt/vol) formaldehyde in PBS supplemented with 0.1% Triton-X (PBS-T), washed three times in PBS-T, and then preblocked for 2–3 h in PBS supplemented with 0.3% Triton-X and 10% (vol/vol) normal goat serum. Brains were incubated overnight in the primary antibody diluted in PBS-T containing 10% (vol/vol) normal goat serum, washed three times with PBS-T, and then incubated with a secondary antibody in PBS-T/10% normal goat serum for 2 h at room temperature. After three further washes in PBS-T, brains were mounted in Vectashield mounting medium containing DAPI (Vectorlabs). The primary antibodies used were mouse anti-β-galactosidase (Promega Z278B, 1:500), rabbit anti-phospho-histone H3 (Cell Signaling Technology 9701, 1:500), mouse anti-V5 (Invitrogen 46–0705, 1:500), mouse anti-DIAP1 (1:400; a gift from Bruce Hay, California Institute of Technology, Pasadena, CA), rabbit anti-Kib [1:100 (8)], guinea pig anti-E2F1 (1:200, a gift from Stefan Thor, Linkoping University, Linkoping, Sweden), rabbit anti-Ex (a gift from Allen Laughon, University of Wisconsin-Madison, Madison, WI; 1:200), rabbit anti-Yki (1:100; a gift from Duojia Pan, Johns Hopkins University, Baltimore), mouse anti-Pros [MR1A, The Developmental Studies Hybridoma Bank (DSHB)], mouse anti-Dl (C594.9B, DSHB) at 1:20, guinea pig anti-Dpn (1:1,000; a gift from James B. Skeath, Washington University School of Medicine, St. Louis), and rat anti-Dpn (1:1; a gift from Cheng-Yu Lee, University of Michigan Medical School, Ann Arbor, MI). The secondary antibodies were goat anti-rat Alexa 647; Alexa 568 goat anti-rabbit, anti-guinea pig, anti-rat, and anti-mouse; and Alexa 488 goat anti-rabbit and anti-mouse (Molecular Probes), all at 1:400.

Image Acquisition and Brain Volume Measurements. Confocal images were acquired on a Zeiss LSM710 confocal laser-scanning microscope using a 40× oil immersion objective lens. A 10× lens was used for whole-brain images. For volume measurements, 3D stacks were acquired at 0.44–0.8-μm intervals. Volume measurements were performed using ImageJ.

Genotypes. Stocks used in this study were *FRT82B lkb1^{x5}/TM6B*, a gift from Jongkyeong Chung, Seoul National University, Seoul, Republic of Korea (65); *UAS-lkb1*, a gift from Bingwei Lu, Stanford School of Medicine, Stanford, CA (94); *FRT82B lkb1^{4A4-2}/TM3* (74) and *FRT42D par-1^{W3}/CyO* (95), gifts from Daniel St. Johnston, University of Cambridge, Cambridge, UK; *FRT82B scrib^{2}*, a gift from Scott Goode, Baylor College of Medicine, Houston; *fj$^{6-11}$* (*fj-lacZ*) and *UAS-yki$^{S11A\ S168A\ S250A}$-V5*, gifts from Ken Irvine, Rutgers University, Piscataway, NJ (39); *ex^{e1} FRT40A/CyO*, a gift from Richard Fehon, University of Chicago, Chicago (96); *ex^{697}* (*ex-lacZ*), a gift from Georg Halder, Vlaams Instituut voor Biotechnologie, Leuven, Belgium; *FRT42D hpo$^{42-47}$/CyO*, a gift from Duojia Pan, Johns Hopkins University, Baltimore; *E(spl)m8-lacZ/CyO*, a gift from Sarah Bray, University of Cambridge, Cambridge, UK; *optix-Gal4*, a gift from Iris Salecker, Medical Research Council National Institute for Medical Research, London; MARCM maker stocks *yw tubGal4 hsFLP122 UAS-nuc-GFP-myc;; FRT82B CD21 y+ tubG80.LL3* and *yw tubGal4 hsFLP122 UAS-nuc-GFP-myc; FRT42D CD21 y+ tubG80.LL3*, gifts from Gary Struhl, Columbia University, New York; and *UAS-yki RNAi^{KK104523}*, *UAS-ampk RNAi^{GD736}*, and *UAS-ampk RNAi^{KK102684}*, from the Vienna *Drosophila* RNAi Centre. Stocks obtained from the Bloomington *Drosophila* Stock Centre are *y w hsFLP;; FRT82B ubi-mRFPnls*; *FRT101 ampk^{3}*; *y w hsFlp FRT101 ubi-GFP*; *P(GawB) NP5443*; *P(GawB)C855a*; *sgt1^{s2383}/TM3*. Other stocks used are *FRT82B UAS-yki^{S168A}-V5/TM6B* (generated by Pedro Gaspar, Francis Crick Institute, London), *UAS-hpo* (30), and *FRT82B wts^{x1}/TM6B* (97).

Generation of *UAS-wts* Transgenic Flies. The *wts* ORF was transferred from the pEntrD-Topo vector (98) into the Gateway-compatible pUASt-attB vector (99), using a LR recombination reaction. Transgenic flies were generated by a site-specific integration at the *attP* site on the third chromosome in the stock *y^{1} w^{1118}; PBac(y^{+}-attP-9)VK00027* (100).

ACKNOWLEDGMENTS. We thank the Vienna Drosophila RNAi Centre, the Bloomington *Drosophila* stock center, the Developmental Studies Hybridoma Bank, and Bestgene Inc for their services. We are grateful to B. Hay, K. Irvine, G. Halder, D. Pan, D. St Johnston, C. Y. Lee, B. Lu, F. Pichaud, P. Gaspar, J. B. Skeath, and S. Thor for stocks and antibodies. We thank C. Berger, K. Harvey, and L. Cheng for discussing data before publication and comments on the manuscript. We are grateful to I. Salecker, H. Apitz, A. Gould, A. Bailey, and C. Berger for helpful advice and reagents. We thank T. Maile for the Flag-Yki expression plasmid. We are thankful to A. Borg and S. Kjaer for protein expression and purification. I. Gailite is supported by European Union Marie Curie fellowship IEF-331192. The N.T. laboratory is supported by Cancer Research UK and the Francis Crick Institute.

1. Yu FX, Guan KL (2013) The Hippo pathway: Regulators and regulations. *Genes Dev* 27(4):355–371.
2. Lin JI, Poon CL, Harvey KF (2013) The Hippo size control pathway–ever expanding. *Sci Signal* 6(259):pe4.
3. Nolo R, Morrison CM, Tao C, Zhang X, Halder G (2006) The bantam microRNA is a target of the hippo tumor-suppressor pathway. *Curr Biol* 16(19):1895–1904.
4. Thompson BJ, Cohen SM (2006) The Hippo pathway regulates the bantam microRNA to control cell proliferation and apoptosis in Drosophila. *Cell* 126(4):767–774.

5. Huang J, Wu S, Barrera J, Matthews K, Pan D (2005) The Hippo signaling pathway coordinately regulates cell proliferation and apoptosis by inactivating Yorkie, the Drosophila Homolog of YAP. *Cell* 122(3):421–434.
6. Tapon N, et al. (2002) salvador Promotes both cell cycle exit and apoptosis in Drosophila and is mutated in human cancer cell lines. *Cell* 110(4):467–478.
7. Neto-Silva RM, de Beco S, Johnston LA (2010) Evidence for a growth-stabilizing regulatory feedback mechanism between Myc and Yorkie, the Drosophila homolog of Yap. *Dev Cell* 19(4):507–520.
8. Genevet A, Wehr MC, Brain R, Thompson BJ, Tapon N (2010) Kibra is a regulator of the Salvador/Warts/Hippo signaling network. *Dev Cell* 18(2):300–308.
9. Cho E, et al. (2006) Delineation of a Fat tumor suppressor pathway. *Nat Genet* 38(10):1142–1150.
10. Hamaratoglu F, et al. (2006) The tumour-suppressor genes NF2/Merlin and Expanded act through Hippo signalling to regulate cell proliferation and apoptosis. *Nat Cell Biol* 8(1):27–36.
11. Harvey KF, Zhang X, Thomas DM (2013) The Hippo pathway and human cancer. *Nat Rev Cancer* 13(4):246–257.
12. Johnson R, Halder G (2014) The two faces of Hippo: Targeting the Hippo pathway for regenerative medicine and cancer treatment. *Nat Rev Drug Discov* 13(1): 63–79.
13. Lian I, et al. (2010) The role of YAP transcription coactivator in regulating stem cell self-renewal and differentiation. *Genes Dev* 24(11):1106–1118.
14. Qin H, et al. (2012) Transcriptional analysis of pluripotency reveals the Hippo pathway as a barrier to reprogramming. *Hum Mol Genet* 21(9):2054–2067.
15. Camargo FD, et al. (2007) YAP1 increases organ size and expands undifferentiated progenitor cells. *Curr Biol* 17(23):2054–2060.
16. Zhang H, Pasolli HA, Fuchs E (2011) Yes-associated protein (YAP) transcriptional coactivator functions in balancing growth and differentiation in skin. *Proc Natl Acad Sci USA* 108(6):2270–2275.
17. Cao X, Pfaff SL, Gage FH (2008) YAP regulates neural progenitor cell number via the TEA domain transcription factor. *Genes Dev* 22(23):3320–3334.
18. Chen Q, et al. (2014) A temporal requirement for Hippo signaling in mammary gland differentiation, growth, and tumorigenesis. *Genes Dev* 28(5):432–437.
19. Cordenonsi M, et al. (2011) The Hippo transducer TAZ confers cancer stem cell-related traits on breast cancer cells. *Cell* 147(4):759–772.
20. Yimlamai D, et al. (2014) Hippo pathway activity influences liver cell fate. *Cell* 157(6): 1324–1338.
21. Mahoney JE, Mori M, Szymaniak AD, Varelas X, Cardoso WV (2014) The hippo pathway effector Yap controls patterning and differentiation of airway epithelial progenitors. *Dev Cell* 30(2):137–150.
22. Shaw RL, et al. (2010) The Hippo pathway regulates intestinal stem cell proliferation during Drosophila adult midgut regeneration. *Development* 137(24):4147–4158.
23. Reddy BV, Rauskolb C, Irvine KD (2010) Influence of fat-hippo and notch signaling on the proliferation and differentiation of Drosophila optic neuroepithelia. *Development* 137(14):2397–2408.
24. Huang J, Kalderon D (2014) Coupling of Hedgehog and Hippo pathways promotes stem cell maintenance by stimulating proliferation. *J Cell Biol* 205(3):325–338.
25. Karpowicz P, Perez J, Perrimon N (2010) The Hippo tumor suppressor pathway regulates intestinal stem cell regeneration. *Development* 137(24):4135–4145.
26. Staley BK, Irvine KD (2010) Warts and Yorkie mediate intestinal regeneration by influencing stem cell proliferation. *Curr Biol* 20(17):1580–1587.
27. Ren F, et al. (2010) Hippo signaling regulates Drosophila intestine stem cell proliferation through multiple pathways. *Proc Natl Acad Sci USA* 107(49):21064–21069.
28. Harvey KF, Pfleger CM, Hariharan IK (2003) The Drosophila Mst ortholog, hippo, restricts growth and cell proliferation and promotes apoptosis. *Cell* 114(4):457–467.
29. Jia J, Zhang W, Wang B, Trinko R, Jiang J (2003) The Drosophila Ste20 family kinase dMST functions as a tumor suppressor by restricting cell proliferation and promoting apoptosis. *Genes Dev* 17(20):2514–2519.
30. Pantalacci S, Tapon N, Léopold P (2003) The Salvador partner Hippo promotes apoptosis and cell-cycle exit in Drosophila. *Nat Cell Biol* 5(10):921–927.
31. Udan RS, Kango-Singh M, Nolo R, Tao C, Halder G (2003) Hippo promotes proliferation arrest and apoptosis in the Salvador/Warts pathway. *Nat Cell Biol* 5(10): 914–920.
32. Wu S, Huang J, Dong J, Pan D (2003) hippo encodes a Ste-20 family protein kinase that restricts cell proliferation and promotes apoptosis in conjunction with salvador and warts. *Cell* 114(4):445–456.
33. Dong J, et al. (2007) Elucidation of a universal size-control mechanism in Drosophila and mammals. *Cell* 130(6):1120–1133.
34. Hao Y, Chun A, Cheung K, Rashidi B, Yang X (2008) Tumor suppressor LATS1 is a negative regulator of oncogene YAP. *J Biol Chem* 283(9):5496–5509.
35. Oka T, Mazack V, Sudol M (2008) Mst2 and Lats kinases regulate apoptotic function of Yes kinase-associated protein (YAP). *J Biol Chem* 283(41):27534–27546.
36. Zhao B, et al. (2007) Inactivation of YAP oncoprotein by the Hippo pathway is involved in cell contact inhibition and tissue growth control. *Genes Dev* 21(21): 2747–2761.
37. Zhang J, Smolen GA, Haber DA (2008) Negative regulation of YAP by LATS1 underscores evolutionary conservation of the Drosophila Hippo pathway. *Cancer Res* 68(8):2789–2794.
38. Oh H, Irvine KD (2008) In vivo regulation of Yorkie phosphorylation and localization. *Development* 135(6):1081–1088.
39. Oh H, Irvine KD (2009) In vivo analysis of Yorkie phosphorylation sites. *Oncogene* 28(17):1916–1927.
40. Piccolo S, Dupont S, Cordenonsi M (2014) The biology of YAP/TAZ: Hippo signaling and beyond. *Physiol Rev* 94(4):1287–1312.
41. Shackelford DB, Shaw RJ (2009) The LKB1-AMPK pathway: Metabolism and growth control in tumour suppression. *Nat Rev Cancer* 9(8):563–575.
42. Hemminki A, et al. (1998) A serine/threonine kinase gene defective in Peutz-Jeghers syndrome. *Nature* 391(6663):184–187.
43. Jenne DE, et al. (1998) Peutz-Jeghers syndrome is caused by mutations in a novel serine threonine kinase. *Nat Genet* 18(1):38–43.
44. Hezel AF, Bardeesy N (2008) LKB1; linking cell structure and tumor suppression. *Oncogene* 27(55):6908–6919.
45. Ji H, et al. (2007) LKB1 modulates lung cancer differentiation and metastasis. *Nature* 448(7155):807–810.
46. Wingo SN, et al. (2009) Somatic LKB1 mutations promote cervical cancer progression. *PLoS One* 4(4):e5137.
47. Sanchez-Cespedes M, et al. (2002) Inactivation of LKB1/STK11 is a common event in adenocarcinomas of the lung. *Cancer Res* 62(13):3659–3662.
48. Calles A, et al. (2015) Immunohistochemical loss of LKB1 is a biomarker for more aggressive biology in KRAS-mutant lung adenocarcinoma. *Clin Cancer Res* 21(12): 2851–2860.
49. Lizcano JM, et al. (2004) LKB1 is a master kinase that activates 13 kinases of the AMPK subfamily, including MARK/PAR-1. *EMBO J* 23(4):833–843.
50. Woods A, et al. (2003) LKB1 is the upstream kinase in the AMP-activated protein kinase cascade. *Curr Biol* 13(22):2004–2008.
51. Shaw RJ, et al. (2004) The tumor suppressor LKB1 kinase directly activates AMP-activated kinase and regulates apoptosis in response to energy stress. *Proc Natl Acad Sci USA* 101(10):3329–3335.
52. Yuan HX, Xiong Y, Guan KL (2013) Nutrient sensing, metabolism, and cell growth control. *Mol Cell* 49(3):379–387.
53. Mohseni M, et al. (2014) A genetic screen identifies an LKB1-MARK signalling axis controlling the Hippo-YAP pathway. *Nat Cell Biol* 16(1):108–117.
54. Nguyen HB, Babcock JT, Wells CD, Quilliam LA (2013) LKB1 tumor suppressor regulates AMP kinase/mTOR-independent cell growth and proliferation via the phosphorylation of Yap. *Oncogene* 32(35):4100–4109.
55. DeRan M, et al. (2014) Energy stress regulates hippo-YAP signaling involving AMPK-mediated regulation of angiomotin-like 1 protein. *Cell Reports* 9(2): 495–503.
56. Mo JS, et al. (2015) Cellular energy stress induces AMPK-mediated regulation of YAP and the Hippo pathway. *Nat Cell Biol* 17(4):500–510.
57. Wang W, et al. (2015) AMPK modulates Hippo pathway activity to regulate energy homeostasis. *Nat Cell Biol* 17(4):490–499.
58. Homem CC, Knoblich JA (2012) Drosophila neuroblasts: A model for stem cell biology. *Development* 139(23):4297–4310.
59. Sousa-Nunes R, Cheng LY, Gould AP (2010) Regulating neural proliferation in the Drosophila CNS. *Curr Opin Neurobiol* 20(1):50–57.
60. Urbach R, Schnabel R, Technau GM (2003) The pattern of neuroblast formation, mitotic domains and proneural gene expression during early brain development in Drosophila. *Development* 130(16):3589–3606.
61. Younossi-Hartenstein A, Nassif C, Green P, Hartenstein V (1996) Early neurogenesis of the Drosophila brain. *J Comp Neurol* 370(3):313–329.
62. Egger B, Boone JQ, Stevens NR, Brand AH, Doe CQ (2007) Regulation of spindle orientation and neural stem cell fate in the Drosophila optic lobe. *Neural Dev* 2:1.
63. Yasugi T, Umetsu D, Murakami S, Sato M, Tabata T (2008) Drosophila optic lobe neuroblasts triggered by a wave of proneural gene expression that is negatively regulated by JAK/STAT. *Development* 135(8):1471–1480.
64. Green P, Hartenstein AY, Hartenstein V (1993) The embryonic development of the Drosophila visual system. *Cell Tissue Res* 273(3):583–598.
65. Lee JH, et al. (2006) JNK pathway mediates apoptotic cell death induced by tumor suppressor LKB1 in Drosophila. *Cell Death Differ* 13(7):1110–1122.
66. Bonaccorsi S, et al. (2007) The Drosophila Lkb1 kinase is required for spindle formation and asymmetric neuroblast division. *Development* 134(11):2183–2193.
67. Bowman SK, et al. (2008) The tumor suppressors Brat and Numb regulate transit-amplifying neuroblast lineages in Drosophila. *Dev Cell* 14(4):535–546.
68. Lee CY, et al. (2006) Drosophila Aurora-A kinase inhibits neuroblast self-renewal by regulating aPKC/Numb cortical polarity and spindle orientation. *Genes Dev* 20(24): 3464–3474.
69. Lee CY, Robinson KJ, Doe CQ (2006) Lgl, Pins and aPKC regulate neuroblast self-renewal versus differentiation. *Nature* 439(7076):594–598.
70. Lee CY, Wilkinson BD, Siegrist SE, Wharton RP, Doe CQ (2006) Brat is a Miranda cargo protein that promotes neuronal differentiation and inhibits neuroblast self-renewal. *Dev Cell* 10(4):441–449.
71. Bello B, Reichert H, Hirth F (2006) The brain tumor gene negatively regulates neural progenitor cell proliferation in the larval central brain of Drosophila. *Development* 133(14):2639–2648.
72. Wang H, et al. (2006) Aurora-A acts as a tumor suppressor and regulates self-renewal of Drosophila neuroblasts. *Genes Dev* 20(24):3453–3463.
73. Richter C, Oktaba K, Steinmann J, Müller J, Knoblich JA (2011) The tumour suppressor L(3)mbt inhibits neuroepithelial proliferation and acts on insulator elements. *Nat Cell Biol* 13(9):1029–1039.
74. Martin SG, St Johnston D (2003) A role for Drosophila LKB1 in anterior-posterior axis formation and epithelial polarity. *Nature* 421(6921):379–384.
75. Goulev Y, et al. (2008) SCALLOPED interacts with YORKIE, the nuclear effector of the hippo tumor-suppressor pathway in Drosophila. *Curr Biol* 18(6):435–441.
76. Nicolay BN, Frolov MV (2008) Context-dependent requirement for dE2F during oncogenic proliferation. *PLoS Genet* 4(10):e1000205.
77. Neumüller RA, et al. (2011) Genome-wide analysis of self-renewal in Drosophila neural stem cells by transgenic RNAi. *Cell Stem Cell* 8(5):580–593.

78. Zhu S, Barshow S, Wildonger J, Jan LY, Jan YN (2011) Ets transcription factor Pointed promotes the generation of intermediate neural progenitors in Drosophila larval brains. *Proc Natl Acad Sci USA* 108(51):20615–20620.
79. Varelas X (2014) The Hippo pathway effectors TAZ and YAP in development, homeostasis and disease. *Development* 141(8):1614–1626.
80. Carney TD, et al. (2012) Functional genomics identifies neural stem cell sub-type expression profiles and genes regulating neuroblast homeostasis. *Dev Biol* 361(1): 137–146.
81. Gold KS, Brand AH (2014) Optix defines a neuroepithelial compartment in the optic lobe of the Drosophila brain. *Neural Dev* 9:18.
82. Badouel C, et al. (2009) The FERM-domain protein Expanded regulates Hippo pathway activity via direct interactions with the transcriptional activator Yorkie. *Dev Cell* 16(3):411–420.
83. Oh H, Reddy BV, Irvine KD (2009) Phosphorylation-independent repression of Yorkie in Fat-Hippo signaling. *Dev Biol* 335(1):188–197.
84. Berger C, et al. (2012) FACS purification and transcriptome analysis of drosophila neural stem cells reveals a role for Klumpfuss in self-renewal. *Cell Reports* 2(2): 407–418.
85. Andersen RO, Turnbull DW, Johnson EA, Doe CQ (2012) Sgt1 acts via an LKB1/AMPK pathway to establish cortical polarity in larval neuroblasts. *Dev Biol* 363(1): 258–265.
86. Mihaylova MM, Shaw RJ (2011) The AMPK signalling pathway coordinates cell growth, autophagy and metabolism. *Nat Cell Biol* 13(9):1016–1023.
87. Hardie DG, Ross FA, Hawley SA (2012) AMPK: A nutrient and energy sensor that maintains energy homeostasis. *Nat Rev Mol Cell Biol* 13(4):251–262.
88. Cheng LY, et al. (2011) Anaplastic lymphoma kinase spares organ growth during nutrient restriction in Drosophila. *Cell* 146(3):435–447.
89. Gumbiner BM, Kim NG (2014) The Hippo-YAP signaling pathway and contact inhibition of growth. *J Cell Sci* 127(Pt 4):709–717.
90. Gordon GM, Zhang T, Zhao J, Du W (2013) Deregulated G1-S control and energy stress contribute to the synthetic-lethal interactions between inactivation of RB and TSC1 or TSC2. *J Cell Sci* 126(Pt 9):2004–2013.
91. Lee JH, et al. (2007) Energy-dependent regulation of cell structure by AMP-activated protein kinase. *Nature* 447(7147):1017–1020.
92. Amin N, et al. (2009) LKB1 regulates polarity remodeling and adherens junction formation in the Drosophila eye. *Proc Natl Acad Sci USA* 106(22):8941–8946.
93. Baas AF, et al. (2004) Complete polarization of single intestinal epithelial cells upon activation of LKB1 by STRAD. *Cell* 116(3):457–466.
94. Wang JW, Imai Y, Lu B (2007) Activation of PAR-1 kinase and stimulation of tau phosphorylation by diverse signals require the tumor suppressor protein LKB1. *J Neurosci* 27(3):574–581.
95. Shulman JM, Benton R, St Johnston D (2000) The Drosophila homolog of C. elegans PAR-1 organizes the oocyte cytoskeleton and directs oskar mRNA localization to the posterior pole. *Cell* 101(4):377–388.
96. Maitra S, Kulikauskas RM, Gavilan H, Fehon RG (2006) The tumor suppressors Merlin and Expanded function cooperatively to modulate receptor endocytosis and signaling. *Curr Biol* 16(7):702–709.
97. Xu T, Wang W, Zhang S, Stewart RA, Yu W (1995) Identifying tumor suppressors in genetic mosaics: The Drosophila lats gene encodes a putative protein kinase. *Development* 121(4):1053–1063.
98. Wehr MC, et al. (2013) Salt-inducible kinases regulate growth through the Hippo signalling pathway in Drosophila. *Nat Cell Biol* 15(1):61–71.
99. Bischof J, Maeda RK, Hediger M, Karch F, Basler K (2007) An optimized transgenesis system for Drosophila using germ-line-specific phiC31 integrases. *Proc Natl Acad Sci USA* 104(9):3312–3317.
100. Venken KJ, He Y, Hoskins RA, Bellen HJ (2006) P[acman]: A BAC transgenic platform for targeted insertion of large DNA fragments in D. melanogaster. *Science* 314(5806):1747–1751.